ELSEVIER

Journal of Power Sources 156 (2006) 655–661

POWER SOURCES

www.elsevier.com/locate/jpowsour

Synthesis of nickel hydroxide: Effect of precipitation conditions on phase selectivity and structural disorder

T.N. Ramesh, P. Vishnu Kamath *

Department of Chemistry, Central College, Bangalore University, Bangalore 560001, India

Received 16 February 2005; accepted 12 May 2005
Available online 14 July 2005

Abstract

The synthesis of nickel hydroxide by precipitation from a suitable solution containing dissolved Ni^{2+} ions is described. A large matrix of precipitation conditions is explored to generate a wide range of nickel hydroxide samples. While most precipitation reactions result in the formation of β-nickel hydroxide, the samples differ from one another in the degree of structural disorder as reflected by the differences in their powder X-ray diffraction (PXRD) patterns. A correlation of the long-range structure as deduced from diffraction studies with the short-range structure as deduced from infrared (IR) spectral studies is performed. The aim is to control the synthesis conditions to obtain materials with 'tailor-made' structural disorders.

Keywords: Nickel hydroxide; Precipitation conditions; Disorder; Non-uniform broadening; Phase selection

1. Introduction

Nickel hydroxide has a low solubility product (1.6×10^{-14}) and is therefore prepared by alkali-induced precipitation from a suitable nickel salt solution. Several factors govern the outcome of a precipitation reaction [1]. Important among these are: (i) pH at precipitation; (ii) choice of alkali; (iii) temperature of the reaction; (iv) choice of the nickel salts; and (v) rate of mixing of the reactants. As in any precipitation reaction, the freshly precipitated nickel hydroxide is digested by ageing in mother liquor, or neutral wash solution or by hydrothermal treatment. Digestion enables crystal growth. Any change in the precipitation conditions affects the structure, composition and morphology of nickel hydroxide with a profound and often unpredictable impact on the reversible charge-storage capacity.

Given the importance of nickel hydroxide to the battery industry, the synthesis of nickel hydroxide has been investigated extensively. Important techniques such as chemical precipitation [2], electrochemical synthesis [3], chimie douce [4], solid-state reactions of nickel acetate with oxalic acid [5], homogeneous precipitation by urea hydrolysis [6], hydrolysis of nickel acetate by a hydrothermal method [7], hydrolysis in polyol medium [8] and others have been used to obtain nickel hydroxide. This study reports the synthesis of nickel hydroxide samples that are obtained by a systematic variation of the precipitation conditions. Each of the samples thus prepared is studied by powder X-ray diffraction (PXRD) and infrared (IR) spectroscopy. The former technique gives the averaged long-range structure, while the short-range coordination is revealed by the IR spectra. The two techniques are thus complementary. Wet chemical analysis provides the chemical composition. Special attention is paid to the line shape of the Bragg reflections in the PXRD pattern as this is indicative of the 'crystallinity' of the sample. An attempt is made to correlate the synthesis conditions to structural disorder with a view to control the synthesis and obtain materials with 'tailor-made' structural disorders.

* Corresponding author. Tel.: +91 80 2296 1331/91 80 2224 5566; fax: +91 80 2293 2685.
E-mail address: vishnukamath8@hotmail.com (P.V. Kamath).

0378-7753/$ – see front matter © 2005 Elsevier B.V. All rights reserved.
doi:10.1016/j.jpowsour.2005.05.050

2. Experimental

2.1. Strong alkali induced precipitation

Nickel hydroxide samples were precipitated by the addition of NaOH (2 M) solution to a solution of nickel nitrate (1 M) at ambient temperature (28–30 °C) using a Metrohm Model 718 STAT Titrino operated in the pH-stat mode. Nickel hydroxide precipitation begins at pH = 5.5–6. In separate experiments, the alkali addition was stopped at final pH values of 7, 9 and 12, respectively, to study the effect of pH on the product. These samples were labelled 7SH, 9SH and 12SH (SH: sodium hydroxide), respectively.

A second set of samples was precipitated at a constant high (>13) pH by the addition of a nickel nitrate solution (1 M, 50 mL) at the rate of 4 mL min^{-1} to a reservoir of NaOH (2 M, 100 mL) that was placed in a thermostat. In separate experiments, the precipitation was carried out at 4, 25 and 80 °C to examine the effect of temperature. These samples are labelled 13SH4, 13SH25 and 13SH80, respectively. To study the effect of digestion, the freshly precipitated 13SH80 slurry was divided into three parts: the first part was immediately filtered, the second aged in mother liquor at 80 °C (18 h), and the third was hydrothermally treated in mother liquor at 170 °C for 48 h (50% filling) in a PTFE lined autoclave.

To study the effect of alkali concentration, a nickel nitrate solution was added to 10 M NaOH (rate of addition of 4 mL min^{-1}). The resultant slurry was divided into two parts: one part was aged in mother liquor for 96 h at 80 °C and the other was hydrothermally treated at 200 °C (48 h). These samples are labelled as CA80 and CA200 (CA: concentrated alkali), respectively.

To study the effect of the nickel source, in separate experiments, nickel sulfate, nickel sulfamate and nickel ammonium sulfate (NAS) were used. In case of NAS, precipitations were performed using stoichiometric quantities of NaOH (final pH 8.2).

13SH80 slurries were aged in 2 and 6 M ammonia solutions for 18 h at 80 °C.

2.2. Ammonia-induced precipitation

Ammonia solution (2 M, 100 mL) was added at the rate of 5 mL min^{-1} to a nickel nitrate (1 M, 50 mL) solution placed in a thermostat. Separate precipitations were carried out at 4, 25 and 65 °C. The resultant slurries were aged in mother liquor for 18–28 h at the respective precipitation temperatures. The samples are labelled as WH4, WH25 and WH65 (WH: weak hydroxide), respectively. Precipitations were also carried out using nickel sulfate, nickel sulfamate and NAS.

The WH4 sample was hydrothermally treated in 6–10 M KOH for 18–48 h at 140–200 °C, besides being aged at ambient temperature for 15 days in 6 M KOH and a 27% (w/v) solution of ammonia.

2.3. Other methods

2.3.1. Removal of ammonia

Ammonia (9 M, 100 mL) was added to nickel nitrate solution (1 M, 50 mL). The initially formed green precipitate redissolves on complete addition with the formation of a deep-blue coloured nickelhexammine complex. The resultant blue solution of $[Ni(NH_3)_6]^{2+}$ was transferred to a vacuum glass dessicator together with a beaker containing concentrated sulfuric acid for 8 days. Slow removal of ammonia from aqueous $[Ni(NH_3)_6]^{2+}$ gave rise to a green solid.

2.3.2. Inter-diffusion method

Slow inter-diffusion of solutions that contain the required ions is known to yield good crystalline materials [9]. Nickel nitrate solution (2 M, 15.4 mL) was added by means of a pipette to the bottom of a 100 mL beaker containing 75 mL of water. This solution together with ammonia (2 M, 150 mL) in a separate beaker was placed in a vacuum glass dessicator. After 2 days, the green-coloured nickel nitrate solution turned into deep blue and a green solid settled at the bottom. After 5 days, a fresh aliquot of ammonia was taken. The final pH of the solution was 9.2.

In all cases, the blue nickelammine complex was formed in addition to a green precipitate of nickel hydroxide. The precipitation was therefore not quantitative.

The precipitates were washed copiously with water and dried at 65–80 °C to constant weight.

2.4. Wet chemical analysis

All nickel hydroxide samples were characterized by wet chemical analysis to arrive at an approximate formula [6]. The nickel content was estimated by the DMG method. The OH^- content was estimated by dissolving a known weight of the sample in excess of acid and back titrating the excess against a standard NaOH solution using a pH meter. In instances of non-stoichiometry, the excess positive charge was made good by the inclusion of anions. The unaccounted weight was attributed to the water content to arrive at an approximate formula given by $Ni(OH)_{2-x}(A^{n-})_{x/n}\cdot zH_2O$. Isothermal decomposition was carried out by heating a known amount of the sample at 700 °C. The weight lost was found to be consistent with the results of wet chemical analysis (product of decomposition, NiO, a = 4.179 Å).

2.5. Characterization

All the samples were characterized by PXRD using either a JEOL Model JDX8P powder diffractometer or a Siemens D5005 diffractometer using a Cu Kα (λ = 1.5418 Å) or a Co Kα (λ =1.7902 Å) source. Infrared spectra were obtained using a Nicolet Model Impact 400D FTIR spectrometer (KBr pellets, resolution 4 cm^{-1}).

3. Results and discussion

Bonding in nickel hydroxide is anisotropic. While intra-layer bonding is strongly iono-covalent in nature, bonding between layers is of the weak van der Waal's type. The layers therefore tend to lose orientation with respect to each other and this results in disorder [10]. The orientation of layers is affected by the precipitation conditions and hence it is important to explore different regimes of pH, concentration and temperature, as well as the conditions of digestion.

3.1. Sodium hydroxide-induced precipitation

3.1.1. Precipitation at constant low pH

Nickel salt solutions tend to be acidic (pH ≈ 3) and on the addition of strong alkali, precipitation takes place at pH = 5.5–6. Terminating alkali addition at pH = 7 yields a sample obtained at a constant 'low pH'. Addition of excess alkali creates the possibility of the interaction of nickel hydroxide with OH^- in solution. Although nickel hydroxide is generally not known to be amphoteric, this interaction appears to affect the structure of the product. The PXRD patterns of 7SH and 12SH samples obtained by strong alkali precipitation at pH 7 and 12, respectively, are shown in Fig. 1. The *d*-spacing of 7SH appear at values expected for β-$Ni(OH)_2$ (PDF: 14–117), but the peaks are non-uniformly broadened. The first peak at 4.64 Å ($2\theta = 19.1^\circ$) corresponds to inter-layer separation in β-$Ni(OH)_2$. The ($h\,k\,0$) peaks, i.e., (1 0 0) and (1 1 0) are the narrowest, whereas the ($h\,0\,\ell$), and (0 0 1) peaks are considerably broadened. The PXRD pattern of 9SH is similar and therefore is not shown.

The high angle (>30° in 2θ) reflections in the PXRD pattern of 12SH appear at positions expected for the β-$Ni(OH)_2$ phase, but the first reflection is poorly defined on account of excessive broadening and due to the appearance of an additional feature. There are two maxima at 5.3 Å (16.7° in 2θ) and 4.64 Å (19.1° in 2θ). Such a pattern was originally ascribed to a phase which is neither α nor β [11], but more recently has been attributed to the interstratification

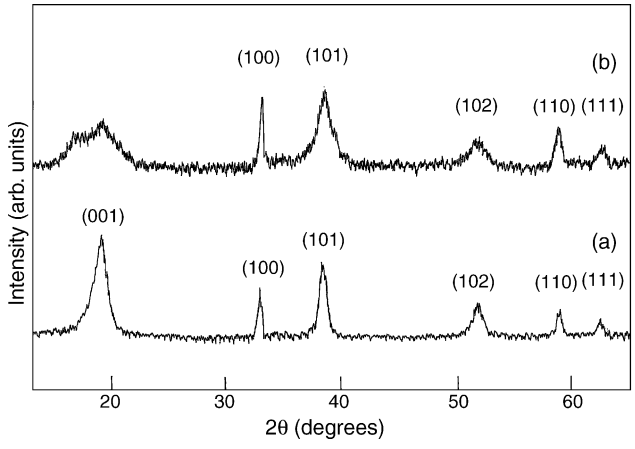

Fig. 1. PXRD patterns for (a) 7SH and (b) 12SH nickel hydroxide samples.

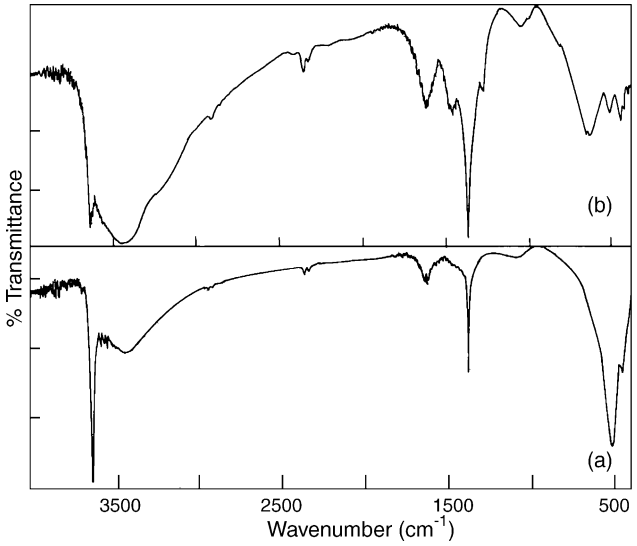

Fig. 2. Infrared spectra for (a) 7SH and (b) 12SH nickel hydroxide samples.

of α-motifs in the matrix of β-$Ni(OH)_2$ [12]. The interstratification model for 12SH is also supported by IR spectra (see Fig. 2).

The spectrum of 7SH shows only three absorptions: (i) a 3650 cm^{-1} peak due to non-hydrogen bonded OH groups; (ii) an in-plane Ni–O–H bending vibration at 520 cm^{-1}; (iii) Ni–O stretching at 460 cm^{-1}.

The sharp peak at 1388 cm^{-1} is due to adsorbed nitrates.

In addition to these absorptions, the spectrum of 12SH shows peaks due to (i) hydrogen-bonded OH stretching at 3450 cm^{-1}; (ii) intercalated nitrate ions in the wave number region 1600–1100 cm^{-1}; (iii) blue-shifted Ni–O–H bending vibration at 640 cm^{-1}. These are characteristic of the α-nickel hydroxide motifs [13].

3.1.2. Precipitation at constant high pH

Precipitation at a constant high pH can be carried out by the addition of nickel nitrate to a reservoir containing NaOH taken in excess. The PXRD pattern of the resultant product (13SH25) is given in Fig. 3, both before and after ageing at

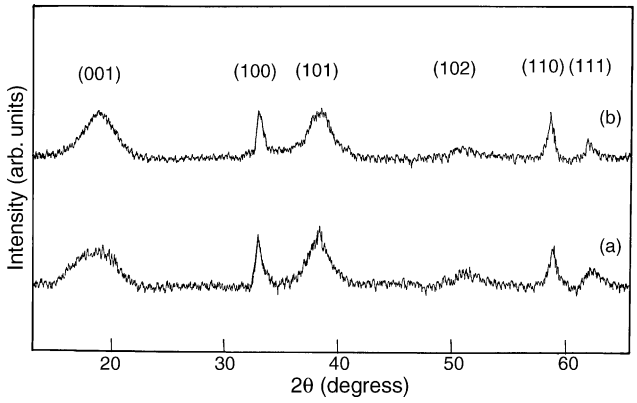

Fig. 3. PXRD patterns for (a) 13SH25 and (b) 13SH80 β-nickel hydroxide samples.

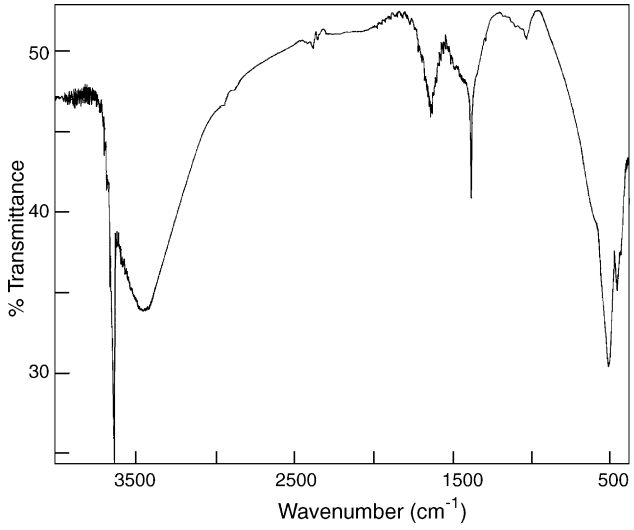

Fig. 4. Infrared spectrum for the 13SH25 nickel hydroxide sample.

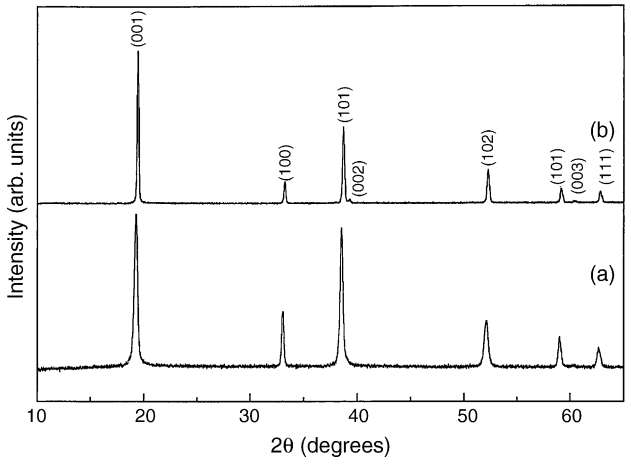

Fig. 5. PXRD patterns for (a) 13SH170 and (b) CA200 β-nickel hydroxide samples.

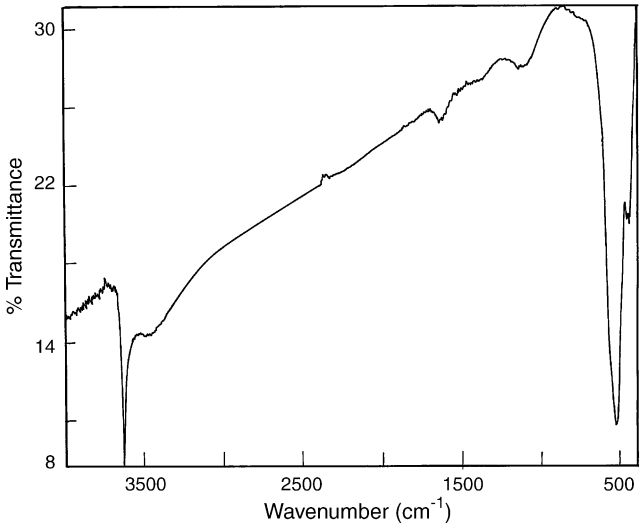

Fig. 6. Infrared spectrum of the CA200 nickel hydroxide sample.

80 °C. This sample is characterized by the excessive broadening of all reflections and near complete extinction of the (1 0 2) reflection. This sample, as reported elsewhere [14], is replete with different types of structural disorder and is known as β_{bc} (bc: badly crystalline)-nickel hydroxide. These disorders are incorporated during the crystallization process and cannot be eliminated by ageing at different temperatures at ambient pressure. Thereby, 13SH4 and 13SH80 have the same features (data not shown). The IR spectrum of 13SH25 is presented in Fig. 4. It differs from that of 12SH by the absence of strong nitrate-related vibrations and by the fact that the 640 cm^{-1} peak is a shoulder to the more prominent 520 cm^{-1}. These features are considered to indicate the presence of intercalated water, but not nitrate ions in β_{bc}-nickel hydroxide. Chemical compositions from wet chemical analysis for the above samples clearly provide additional evidence (see Table 1). The 12SH is a material deficient in hydroxyl ions and requires the inclusion of nitrates for charge neutrality. 13SH25 is a stoichiometric phase with a $[Ni^{2+}]/[OH^-]$ ratio of 0.5.

When 13SH slurry is hydrothermally treated at 170 °C, it undergoes dramatic ordering to yield a highly crystalline sample (see Fig. 5(a)), in which non-uniform broadening is completely eliminated. On the other hand, the peaks corresponding to the $(h\,0\,\ell)$ reflections have broad wings at the base. Further narrowing of the peaks and elimination of the wings is seen in the CA200 sample (Fig. 5(b)). The orientation of the layers is so good as to give rise to the (0 0 2) and (0 0 3) reflections (39° and 60.44° in 2θ). The IR spectrum of the CA200 sample shown in Fig. 6 is the one ideally expected for β-$Ni(OH)_2$ [15].

The crystallinity of the product is adversely affected on using a non-nitrate source. The PXRD pattern of nickel hydroxide obtained from nickel sulfate is given in Fig. 7(a) and that for the product obtained from a reaction of NAS with a stoichiometric requirement of NaOH (final pH = 8.2) in Fig. 7(b). This latter sample is X-ray amorphous. The IR spectrum is presented in Fig. 8 and it exhibits all the features

Table 1
Wet chemical analysis of nickel hydroxide samples

Sample	Wet chemical analysis (wt.%)				Approximate formula	Total weight loss (%)[a]
	Ni^{2+}	OH^-	NO_3^-	H_2O		
12SH	48.9	26	8.3	16.7	$Ni(OH)_{1.84}(NO_3)_{0.16}\cdot 1.1H_2O$	32.6 (37.6)
13SH25	54.34	31.84	–	13.70	$Ni(OH)_2\cdot 0.83H_2O$	33 (31.3)

[a] Values in parentheses are calculated on basis of approximate formulae.

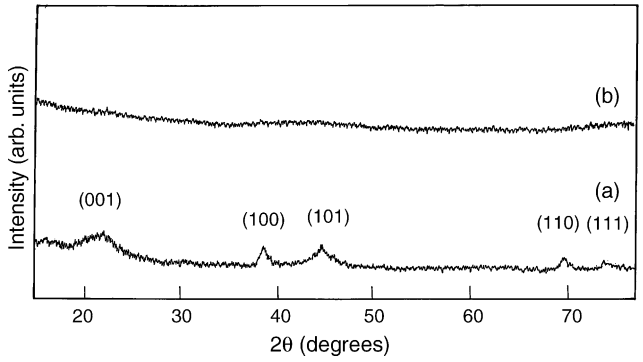

Fig. 7. PXRD patterns for nickel hydroxide samples obtained from (a) nickel sulfate and (b) NAS.

expected of the α-modification of nickel hydroxide, namely: (i) a hydrogen-bonded OH stretching at 3430 cm^{-1}; (ii) a peak at 1120 cm^{-1} due to the intercalated sulphate ions; (iii) a blue shifted Ni–O–H bending vibration at 620 cm^{-1}.

The first coordination shell around Ni in the sample is similar to that in α-nickel hydroxide.

Interstratified nickel hydroxide is obtained from NAS at pH = 13. Nickel sulfamate yields a sample similar to that of 13SH80 (data not shown).

In an attempt to induce ordering, the β_{bc} slurry of 13SH80 was aged in ammonia solutions (2 and 6 M). The results are shown in Fig. 9. Progressive narrowing of the peaks is discernible and in Fig. 9(a), narrow peaks are seen to arise on a broad base. The pattern appears to be a convolution of the peaks due to two phases: one is a disordered phase while the other is crystalline. The ordering has considerably improved in Fig. 9(b) although the broad wings under the (1 0 1) reflection persist. Such a line shape has been attributed to crystallites with stacking faults [16]. Fig. 9 also shows that the rate of ordering increases when the concentration of ammonia increases.

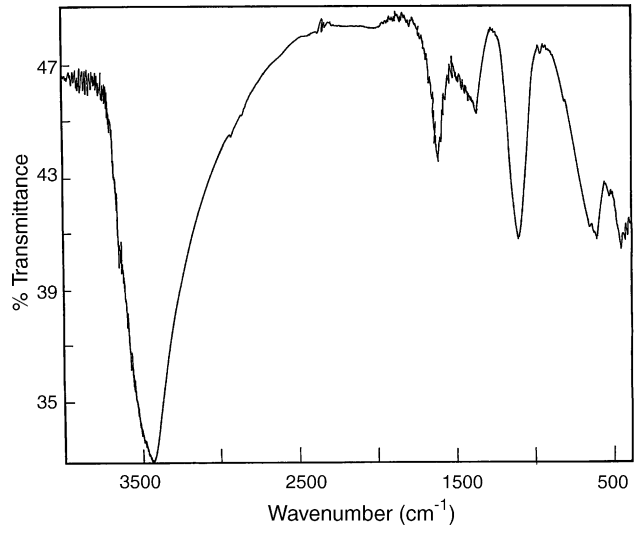

Fig. 8. Infrared spectrum for sample corresponding to Fig. 7(b).

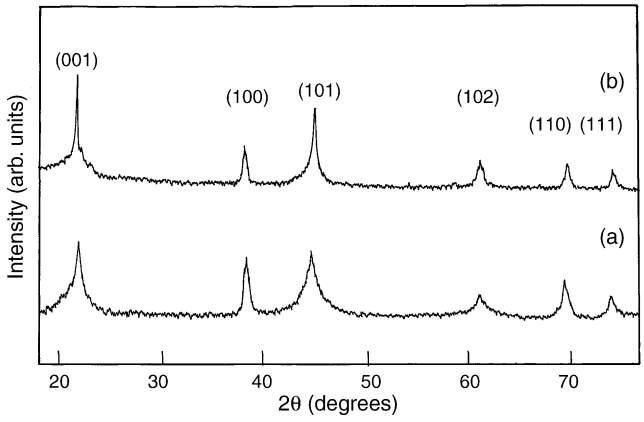

Fig. 9. PXRD pattern for 13SH80 slurry aged in (a) 2 M NH_3 and (b) 6 M NH_3.

3.2. Ammonia-induced precipitation

Ammonia-induced precipitation at low temperature (4 °C), WH4, yields a poorly ordered α-nickel hydroxide, while at high temperature (25–65 °C), β-$Ni(OH)_2$ is obtained with a surprisingly high degree of crystallinity (Fig. 10). The PXRD pattern of WH4 (Fig. 10(a)) is characteristic of a material with turbostratic disorder [13]. The two high-angle reflections are accordingly indexed to reflect the two-dimensional ordering of nickel hydroxide sheets. The low-angle reflection appearing at 7.6 Å corresponds to the inter-layer spacing in α-nickel hydroxide. The IR spectra also reflect the dramatic changes brought about by the change in temperature (Fig. 11). WH4 exhibits all the characteristic absorptions of α-nickel hydroxide, while WH25 shows the features of β-$Ni(OH)_2$.

When α-nickel hydroxide (WH4) is aged in concentrated ammonia at ambient temperature, it transforms into crystalline β-$Ni(OH)_2$ (see Fig. 12(a) for the PXRD pattern of a partially-transformed sample). On ageing in concentrated alkali (6 M KOH), it transforms into β_{bc}-nickel hydroxide (Fig. 12(b)). This clearly shows that the pH during ageing has a profound affect on structural disorder.

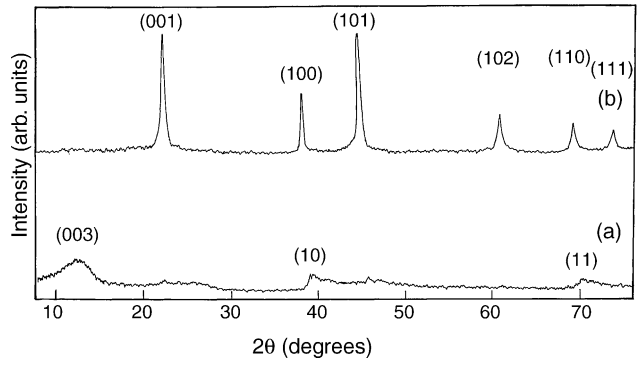

Fig. 10. PXRD pattern of (a) WH4 sample compared with that of (b) WH25 sample.

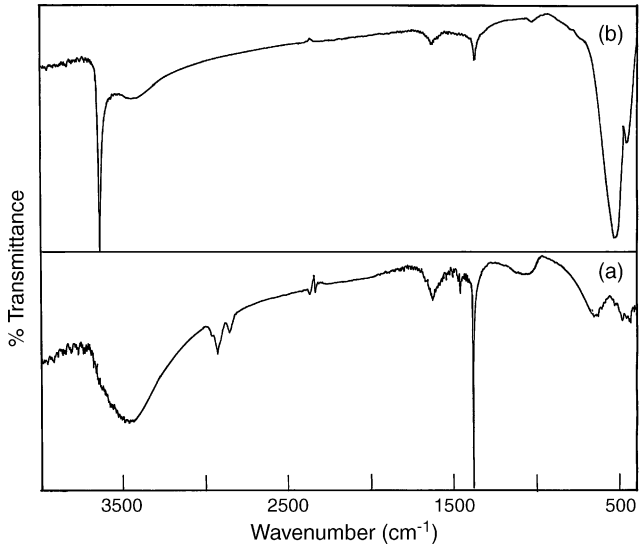

Fig. 11. Infrared spectra for (a) WH4 sample and (b) WH25 nickel hydroxide samples.

3.3. Disorder → Order transformation in nickel hydroxide system

Precipitation of a solid takes place when two solutions having different free energies are mixed [17]. According to Ostwald's law [18], the solid obtained immediately on precipitation is not only disordered but also thermodynamically unstable with a free energy close to that of the reactants. The disordered phase transforms into a more stable phase of lower free energy in a step-wise manner. During the precipitation of nickel hydroxide, especially at low temperatures and moderate pH conditions as obtained during ammonia induced precipitations or stoichiometric strong alkali addition, the solid formed immediately on precipitation is the α-amorphous phase. This phase is metastable and transforms into other phases of progressively greater order and thermodynamic stability. Our observations show that the transformation takes place as:

$$\alpha\text{-amorphous} \rightarrow \beta_{bc} \rightarrow \beta\text{-nickel hydroxide.} \quad (1)$$

In strong alkali, once the first step is completed (as in Fig. 12(b)), further transformation becomes very slow and can be accelerated only at high alkali concentrations (>10 M) and/or high temperature (>80 °C). A long (18–96 h) duration is also needed to complete the transformation (as in Fig. 5). All these conditions point to dissolution–reprecipitation as the possible mechanism for the second step. The poor amphotericity of nickel hydroxide demands harsh conditions for the transformation to occur. In ammonia, however the solubility of $Ni(OH)_2$ can be enhanced, therefore the $\beta_{bc} \rightarrow \beta$ transformation takes place under relatively milder conditions (NH_3 concentration 6 M, 28–30 °C, 18 h) due to an interplay of the following equilibria:

$$\beta_{bc}\text{-}Ni(OH)_2 + 6NH_4(OH) \Leftrightarrow [Ni(NH_3)_6]^{2+} + 6H_2O + 2OH^- \quad (2)$$

$$[Ni(NH_3)_6]^{2+} \Leftrightarrow Ni^{2+} + 6NH_3 \quad (3)$$

$$6NH_3 + 6H_2O \Leftrightarrow 6NH_4(OH) \quad (4)$$

$$Ni^{2+} + 2OH^- \Leftrightarrow \beta\text{-}Ni(OH)_2 \quad (5)$$

The dissolution–reprecipitation reaction is driven by free energy changes at the solid|solution interface. The surface layers of β_{bc} nickel hydroxide interact strongly with the solution and their contribution to the free energy of the crystallite is small. This is especially true in instances where the nickel coordination is either incomplete or asymmetric as in the case of interstratified and hydroxyl-deficient samples. The surface layers therefore dissolve. When they reprecipitate, the slow kinetics leads to better crystallization and the surface layers are strongly bound to the ordered crystallite so that their contribution to the free energy of the crystallite exceeds the strength of interaction with the solution. For similar reasons, the inter-diffusion method, as well as the removal of ammo-

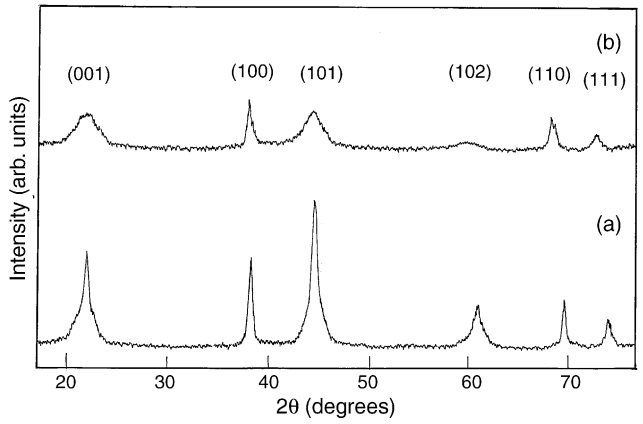

Fig. 12. PXRD pattern for WH4 sample aged in (a) 27% (w/v) NH_3 and (b) 6 M KOH for 15 days.

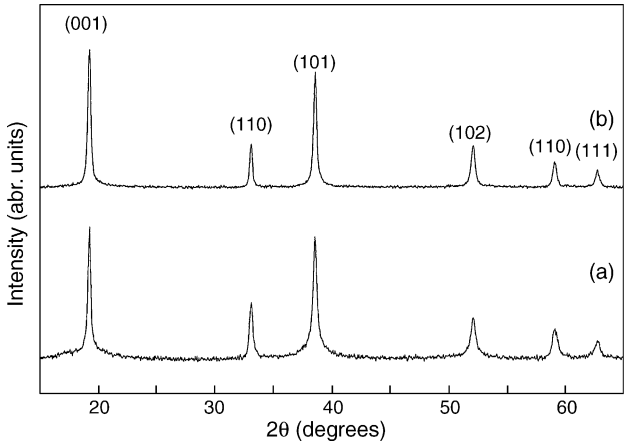

Fig. 13. PXRD patterns for β-nickel hydroxide samples obtained by (a) removal of ammonia and (b) diffusion methods.

nia method, lead to the formation of crystalline samples (see Fig. 13). In the former method, ammonia has been introduced slowly with the object of forming the nickelammine complex in situ followed by hydrolysis. The latter method starts from the complex and facilitates precipitation by controlled decomposition of the complex by the slow removal of ammonia.

4. Conclusion

Nickel hydroxide samples have been prepared under a variety of precipitation conditions and characterized by PXRD and IR spectroscopy. From an empirical examination of the PXRD data, the samples prepared appear to have different amounts of structural disorder. Ageing freshly precipitated slurries brings about changes in the long-range as well as short-range structure of nickel hydroxide.

Acknowledgements

PVK is grateful to the Department of Science and Technology, Government of India (GOI) for financial support. TNR thanks the Council of Scientific and Industrial Research, GOI for the award of a Senior Research Fellowship (NET). The authors wish to acknowledge help from the Solid State and Structural Chemistry Unit, Indian Institute of Science in providing powder X-ray diffraction facilities.

References

[1] R.P. Grosso, S.L. Suib, R.S. Weber, P.F. Schubert, Chem. Mater. 4 (1992) 922–928.
[2] C. Zhaorong, L. Gongan, Z. Yujuan, C. Jianguo, C. Jianguo, D. Yunchang, J. Power Sources 74 (1998) 250–254.
[3] E.J. McHenry, Electrochem. Technol. 5 (1967) 275–277.
[4] J.J. Braconnier, C. Delmas, C. Fouassier, M. Figlarz, B. Beaudouin, P. Hagenmuller, Rev. Chim. Miner. 21 (1984) 496–508.
[5] X. Liu, L. Yu, Mater. Lett. 58 (2004) 1327–1330.
[6] M. Dixit, G.N. Subbanna, P.V. Kamath, J. Mater. Chem. 6 (1996) 1429–1432.
[7] H. Nishizama, T. Kishikawa, H. Minami, J. Solid State Chem. 146 (1999) 39–46.
[8] L. Poul, N. Jouini, F. Fievet, Chem. Mater. 12 (2000) 3123–3132.
[9] Y.M. De Hann, Nature 200 (1963) 876.
[10] A.-C. Gaillot, D. Flot, V.A. Drits, A. Manceau, M. Burghammer, B. Lanson, Chem. Mater. 15 (2003) 4666–4678.
[11] M. Rajamathi, G.N. Subbanna, P.V. Kamath, J. Mater. Chem. 7 (1997) 2293–2296.
[12] M. Rajamathi, P.V. Kamath, R. Seshadri, J. Mater. Chem. 10 (2000) 503–506.
[13] P. Oliva, J. Leonardi, J.F. Laurent, C. Delmas, J.J. Braconnier, M. Figlarz, F. Fievet, A. de Guibert, J. Power Sources 8 (1982) 229–255.
[14] T.N. Ramesh, R.S. Jayashree, P.V. Kamath, Clay Clay Miner. 51 (2003) 570–576.
[15] S.S. Mitra, Z. Kristall. 116 (1961) 149–153.
[16] C. Delmas, C. Tessier, J. Mater. Chem. 7 (1997) 1439–1442.
[17] J.J. De Voreo, P.G. Vekilov, in: P.M. Dove, J.J. De Voreo, S. Weiner (Eds.), Reviews in Minerology and Geochemistry, Minerological Society of America, Washington, DC, 2003.
[18] W. Ostwald, Z. Physk. Chem. 22 (1897) 289 as quoted in: A.R. Verma, P. Krishna, Polymorphism and Polytypism in Crystals, John Wiley and Sons, New York, USA, 1966, p. 33.